

Mixed convection boundary layer flow from a vertical truncated cone in a nanofluid

F.O. Pătrulescu^a, T. Groșan^{b*}, I. Pop^b

^a”Tiberiu Popoviciu” Institute of Numerical Analysis of Romanian Academy, Cluj-Napoca, Romania

^b Babeș -Bolyai University, Department of Mathematics, Cluj-Napoca, Romania

Abstract

Purpose – In this paper we investigate the steady mixed convection boundary layer flow from a vertical frustum of a cone in water-based nanofluids. The problem is formulated to incorporate three kinds of nanoparticles: Copper (Cu), Alumina (Al_2O_3) and Titanium oxide (TiO_2). The working fluid is chosen as water with the Prandtl number of $Pr = 6.2$. The mathematical model used for the nanofluid incorporates the particle volume fraction parameter, the effective viscosity and the effective thermal diffusivity. The entire regime of the mixed convection includes the mixed convection parameter λ , which is positive for the assisting flow (heated surface of the frustum cone) and negative for the opposing flow (cooled surface of the frustum cone), respectively.

Design/methodology/approach – The transformed nonlinear partial differential equations are solved numerically for some values of the governing parameters. The derivatives with respect to ξ were discretized using the first order upwind finite differences and the resulting ordinary differential equations with respect to η were solved using *bvp4c* routine from Matlab. The absolute error tolerance in *bvp4c* was $1e-9$.

Findings – The features of the flow and heat transfer characteristics for different values of the governing parameters are analysed and discussed. The effects of the particle volume fraction parameter ϕ , the mixed convection parameter λ and the dimensionless coordinate ξ on the flow and heat transfer characteristics are determined only for the Cu nanoparticles. It is found that dual solutions exist for the case of opposing flows. The range of the mixed convection parameter for which the solution exists increases in the presence of the nanofluids.

Originality/value – The paper models the mixed convection from a vertical truncated cone using the boundary layer approximation. Multiple (dual) solutions for the flow reversals are obtained and the range of existence of the solutions was found. Particular cases for $\xi = 0$ (full cone), $\xi \gg 1$ and $\lambda \gg 1$ (free convection limit) were studied. To the authors best knowledge this problem has not been studied before and the results are new and original.

Keywords Truncated cone, Boundary layer, Mixed convection, Nanofluids, Numerical results, Dual solutions

Paper type Research paper

***Corresponding author**

Dr. T. Grosan can be contacted at: tgrosan@math.ubbcluj.ro

Nomenclature

C_f	skin friction coefficient
-------	---------------------------

C_p	specific heat at constant pressure
$f(\eta)$	similarity variable
g	acceleration due to gravity
Gr_x	local Grashof number
k	thermal conductivity of the nanofluid
Nu_x	local Nusselt number
Pr	Prandtl number
q_w	heat flux from the surface of the cone
r	radial distance
Re_x	local Reynolds number
T	temperature of the nanofluid
T_w	wall temperature
T_∞	temperature of the ambient nanofluid
u, v	velocity components along x and y directions, respectively
U_∞	characteristic velocity
x, y	Cartesian coordinates measured along the surface of the truncated cone and normal to it, respectively
x_0	distance measured from the leading edge of the truncated cone

Greek letters

α	thermal diffusivity
β	thermal expansion coefficient
φ	particle volume fraction
η	similarity variable
λ	mixed convection parameter
λ_{cr}	critical value of λ
μ	dynamic viscosity
ν	kinematic viscosity
$\theta(\eta)$	dimensionless temperature
ρ	density
τ_w	skin friction or shear stress
ξ	dimensionless variable
ψ	stream function

Subscripts

nf	nanofluid
f	base fluid
s	solid particle

1. Introduction

Convective heat transfer is present in many engineering processes such as thermal powerplants, heat exchangers, environmental comfort, energy storage systems and electronic cooling. Fluids such as oil, water and ethylene glycol mixture are poor heat transfer fluids, since the thermal conductivity of these fluids, which is generally small, play important role on the heat transfer coefficient between the heat transfer medium and the heat transfer surface. The term nanofluid refers to a liquid containing (e.g. water, ethylene glycol, engine oils, etc.) a suspension of solid particles (nanoparticles) in conventional heat transfer fluids. It seems that Choi (1995) is the first who used the term nanofluids to refer to the fluid with suspended nanoparticles. Nanoparticles can be metallic particles such as those of Cu, Ag, Au, etc. or metallic oxides or non-metallic oxide particles: CuO, Al₂O₃, TiO, SiO, etc. having dimensions in the range 1 to 100nm. Significant features of nanofluids over base fluids include enhanced thermal conductivity, greater viscosity, and enhanced value of critical heat flux. Of these the most talked about is the enhanced thermal conductivity, a phenomenon which was first reported by Masuda et al. (1993), Ding et al. (2007) reported the use of nanofluids in a wide variety of industries ranging from transportation, heating, ventilation, and air conditioning (HVAC), and energy production and supply to electronics, textiles, paper production, etc. It is worth to mention that there are several patents which use nanofluids in heat transfer problems such as heat pumps and solar energy collectors (see, LaForgia et al. 2013 and Olson, 2013). Choi et al. (2001) showed that the addition of a small amount (less than 1% by volume) of nanoparticles to conventional heat transfer liquids increased the thermal conductivity of the fluid up to approximately two times. Therefore, the effective thermal conductivity of nanofluids is expected to enhance heat transfer compared with conventional heat transfer liquids (Masuda et al., 1993). All of these industries deal with heat transfer in some or the other way, and thus have a strong need for improved heat transfer mediums. This could possibly be nanofluids, because of some potential benefits over normal fluids— large surface area provided by nanoparticles for heat exchange, reduced pumping power due to enhanced heat transfer, minimal clogging, innovation of miniaturized systems leading to savings of energy and cost. Choi's (1995) results have been supported by other researchers from time to time. Eastman et al. (2001) reported an increase of 40% in the effective thermal conductivity of ethylene-glycol with 0.3% volume of copper nanoparticles of 10nm diameter. Further 10-30% increase of the effective thermal conductivity in alumina/water nanofluids with 1-4% of alumina was reported by Das et al. (2003). Buongiorno and Hu (2005) suggested the possibility of using nanofluids in advanced nuclear

systems. Another recent application of the nanofluid flow is in the delivery of nano-drug as suggested by Kleinstreuer et al. (2008).

A comprehensive survey of convective transport in nanofluids was made by Buongiorno (2006), Choi (2009), Kakaç and Pramuanjaroenkij (2009), Das and Choi (2009), Fan and Wang (2011), etc. We have also mentioned the valuable published books by Das et al. (2007) and Schaefer (2009). Buongiorno (2006) has pointed out that the nanoparticle absolute velocity can be viewed as the sum of the base fluid velocity and a relative velocity (that he calls the slip velocity). He considered in turn seven slip mechanisms: inertia, Brownian diffusion, thermophoresis, diffusiophoresis, Magnus effect, fluid drainage, and gravity settling (Nield and Kuznetsov, 2009). Numerous models and methods have been proposed by different authors to study convective flows of nanofluids and we mention here the papers by Khanafer et al. (2003), Tiwari and Das (2007), Oztop and Abu-Nada (2008), Rohni et al. (2009), Mansur et al. (2009), Nield and Kuznetsov (2010), Kuznetsov and Nield (2010), Tham et al. (2012), Aminossadati and Ghasemi (2012), etc.

The problem of viscous boundary-layer flow on a full and truncated cone is a classical problem, and it has been considered by many researchers, for example Chiou and Na (1980), Kumari et al. (1989), Chamkha (2001), Molla et al. (2009), Mahdy et al. (2010), Chamkha and Rashad (2012), Chamkha et al. (2012), etc. Engineering applications of this particular geometry (truncated cone) are in the field of heat exchangers, cooling of electronic devices, etc. (see Shinmura, 1996; Hamilton et al. 1999; McCutcheon et al., 2005 and Nakamura et al., 2010).

Different from the previous investigations, following the nanofluid equations model proposed by Tiwari and Das (2007), we consider in this paper the development of the steady mixed convection boundary-layer flow on a vertical impermeable frustum of a cone in a nanofluid. The problem is formulated so that we can consider three different types of nanoparticles, namely Cu (copper), Al_2O_3 (alumina) and TiO_2 (titania), and water as a base fluid. However, in order to save space, we have considered here only the case of Cu nanoparticles. The motivation for this study is that nanotechnology has been widely used in industry because materials with sizes of nanometers possess unique physical properties. The dimensionless governing partial differential equations have been solved numerically and the results for the particular case of the full cone have been compared with results reported by Kumari et al. (1989). The results are in very good agreement.

2. Basic equations

Consider the steady mixed boundary layer flow near a vertical truncated cone (with half angle ϕ) as shown in Fig. 1 in a water-based nanofluid. The origin O of the coordinate system is placed at the vertex of the full cone, where x is the co-ordinate measured from the origin O along the surface of the full cone and y is the coordinate normal to the surface of the truncated cone, respectively. The distance of the leading edge of the truncated cone measured from the origin O is denoted as x_0 . The surface of the truncated cone is held at a constant temperature T_w , while the temperature of the ambient nanofluid is T_∞ with $T_w > T_\infty$ for a heated truncated cone (assisting flow) and $T_w < T_\infty$ for a cooled truncated cone (opposing flow), respectively. The velocity far away from the truncated cone in the vertical direction is U_∞ and the viscous dissipation is assumed to be negligible.

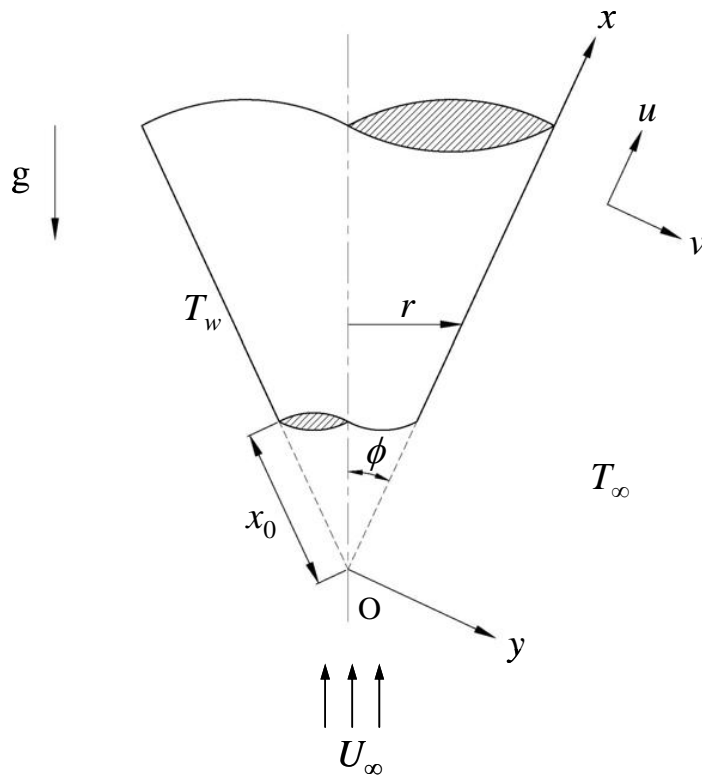


Figure 1. Physical model and coordinate system.

Under the above assumptions along with the assumptions of Boussinesq and boundary layer approximations, the basic equations governing the steady mixed convection boundary layer flow of a

nanofluid near a vertical frustum of a cone can be written as in Chamkha and Rashad (2012) or Pop and Ingham (2001) combined with the mathematical nanofluid model given by Tiwari and Das (2007):

$$\frac{\partial}{\partial x}(ru) + \frac{\partial}{\partial y}(rv) = 0 \quad (1)$$

$$u \frac{\partial u}{\partial x} + v \frac{\partial u}{\partial y} = \frac{\mu_{nf}}{\rho_{nf}} \frac{\partial^2 u}{\partial y^2} + \frac{(\rho\beta)_{nf}}{\rho_{nf}} g (T - T_\infty) \sin \phi \quad (2)$$

$$u \frac{\partial T}{\partial x} + v \frac{\partial T}{\partial y} = \alpha_{nf} \frac{\partial^2 T}{\partial y^2} \quad (3)$$

along with the boundary conditions

$$\begin{aligned} v = 0, \quad u = 0, \quad T = T_w \quad \text{at} \quad y = 0 \\ u = U_\infty, \quad T = T_\infty \quad \text{as} \quad y \rightarrow \infty \end{aligned} \quad (4)$$

where u and v are the velocity components along x and y axes, respectively, T is the temperature of the nanofluid, g is the gravity acceleration, U_∞ is the constant velocity of the outer (inviscid) flow, $r = x \sin \phi$, ρ_{nf} is the effective density, μ_{nf} is the effective dynamic viscosity, $(\rho\beta)_{nf}$ is the thermal expansion coefficient and α_{nf} is the thermal diffusivity of the nanofluid, which are given as (see Khanafer et al., 2003, and Oztop and Abu-Nada, 2008),

$$\begin{aligned} \rho_{nf} = (1 - \phi) \rho_f + \phi \rho_s, \quad \mu_{nf} = \frac{\mu_f}{(1 - \phi)^{2.5}} \\ (\rho\beta)_{nf} = (1 - \phi)(\rho\beta)_f + \phi(\rho\beta)_s, \quad \alpha_{nf} = \frac{k_{nf}}{(\rho C_p)_{nf}} \end{aligned} \quad (5)$$

Here, ϕ is the solid volume fraction, μ_f is the dynamic viscosity of the basic fluid, ρ_f and ρ_s are the densities of pure fluid and nanoparticles, respectively, $(\rho C_p)_{nf}$ is the heat capacity of the nanofluid and k_{nf} is the thermal conductivity of the nanofluid given by

$$(\rho C_p)_{nf} = (1 - \phi)(\rho C_p)_f + \phi(\rho C_p)_s, \quad \frac{k_{nf}}{k_f} = \frac{k_s + 2k_f - 2\phi(k_f - k_s)}{k_s + 2k_f + 2\phi(k_f - k_s)} \quad (6)$$

where $(\rho C_p)_f$ and $(\rho C_p)_s$ are the specific heat parameters of the base fluid and nanoparticles and k_f and k_s are the thermal conductivities of the base fluid and nanoparticles. The viscosity of the nanofluid μ_{nf} can be approximated as the viscosity of a base fluid μ_f containing dilute suspension of fine spherical particles and is given by Brinkman (1952). The effective thermal conductivity of the nanofluid

k_{nf} is approximated by the Maxwell-Garnett's model, which is found to be appropriate for studying heat transfer enhancement using nanofluids (Khanafar et al., 2003; Maïga et al., 2004, etc.).

Further, we introduce the following non-similarity variables

$$\begin{aligned}\xi = \bar{x}/x_0 = (x-x_0)/x_0, \quad \eta = \text{Re}_x^{1/2} (y/\bar{x}), \quad \psi = \text{Re}_x^{1/2} \nu_f r f(\xi, \eta) \\ \theta(\xi, \eta) = (T - T_\infty)/(T_w - T_\infty)\end{aligned}\quad (7)$$

where $\bar{x} = x - x_0$, ν_f is the kinematic viscosity of the based fluid, $\text{Re}_x = U_\infty \bar{x} / \nu_f$ is the local Reynold number and ψ is the stream function, which is defined as

$$ru = \frac{\partial \psi}{\partial y}, \quad rv = -\frac{\partial \psi}{\partial x} \quad (8)$$

Substituting (7) and (8) into Eqs. (2) and (3), we obtain the following partial differential equations of parabolic type

$$\begin{aligned}\frac{1}{(1-\phi)^{2.5} [(1-\phi) + \phi \rho_s / \rho_f]} \frac{\partial^3 f}{\partial \eta^3} + \left(\frac{1}{2} + \frac{\xi}{1+\xi} \right) f \frac{\partial^2 f}{\partial \eta^2} \\ + \frac{(1-\phi) + \phi (\rho \beta)_s / (\rho \beta)_f}{(1-\phi) + \phi \rho_s / \rho_f} \lambda \theta = \xi \left(\frac{\partial f}{\partial \eta} \frac{\partial^2 f}{\partial \xi \partial \eta} - \frac{\partial f}{\partial \xi} \frac{\partial^2 f}{\partial \eta^2} \right)\end{aligned}\quad (9)$$

$$\begin{aligned}\frac{1}{\text{Pr}} \frac{k_{nf}/k_f}{(1-\phi) + \phi (\rho C_p)_s / (\rho C_p)_f} \frac{\partial^2 \theta}{\partial \eta^2} + \left(\frac{1}{2} + \frac{\xi}{1+\xi} \right) f \frac{\partial \theta}{\partial \eta} \\ = \xi \left(\frac{\partial f}{\partial \eta} \frac{\partial \theta}{\partial \xi} - \frac{\partial f}{\partial \xi} \frac{\partial \theta}{\partial \eta} \right)\end{aligned}\quad (10)$$

and the boundary conditions (6) become

$$\begin{aligned}f = 0, \quad \frac{\partial f}{\partial \eta} = 0, \quad \theta = 1 \quad \text{at} \quad \eta = 0 \\ \frac{\partial f}{\partial \eta} = 1, \quad \theta = 0 \quad \text{as} \quad \eta \rightarrow \infty\end{aligned}\quad (11)$$

where λ is the constant mixed convection parameter, which is given by

$$\lambda = \frac{Gr}{\text{Re}_x^2} \quad (12)$$

with $Gr_x = g \beta_f (T_w - T_\infty) x^3 \sin \phi / \nu_f^2$ being the local Grashof number. It should be stated that $\lambda > 0$ ($T_w > T_\infty$) corresponds to a heated truncated cone (assisting flow), $\lambda < 0$ ($T_w < T_\infty$) corresponds to a

cooled truncated cone (opposing flow) and $\lambda = 0$ ($T_w = T_\infty$) corresponds to the forced convection flow along the truncated cone, respectively. Using (7) and (8), the velocity components u and v are given by

$$u = U_\infty \frac{\partial f}{\partial \eta}, \quad v = -\frac{v_f \text{Re}_x^{1/2}}{x} \left[\left(\frac{1}{2} + \frac{\xi}{1+\xi} \right) f + \xi \frac{\partial f}{\partial \xi} - \frac{\eta}{2} \frac{\partial f}{\partial \eta} \right] \quad (13)$$

The quantities of physical interest are also the skin friction coefficient C_f and the local Nusselt number Nu_x which are defined as

$$C_f = \frac{2\tau_w}{\rho_f U_\infty^2}, \quad Nu_x = \frac{x q_w}{k_f (T_w - T_\infty)} \quad (14)$$

where τ_w is the wall skin friction and q_w is the heat flux from the surface of the truncated cone, which are given by

$$\tau_w = \mu_{nf} \left(\frac{\partial u}{\partial y} \right)_{y=0}, \quad q_w = -k_{nf} \left(\frac{\partial T}{\partial y} \right)_{y=0} \quad (15)$$

Using relations (7) in (15) and (14), we obtain

$$\text{Re}_x^{1/2} C_f = \frac{2}{(1-\varphi)^{2.5}} \frac{\partial^2 f}{\partial \eta^2}(\xi, 0), \quad \text{Re}_x^{-1/2} Nu_x = -\frac{k_{nf}}{k_f} \frac{\partial \theta}{\partial \eta}(\xi, 0) \quad (16)$$

The following two particular cases are also of interest:

i) Full cone ($\xi = 0$)

In this case, Eqs. (9) and (10) reduce to the following ordinary differential equations

$$\frac{1}{(1-\varphi)^{2.5} \left[(1-\varphi) + \varphi \rho_s / \rho_f \right]} f'''' + \frac{1}{2} f f'' + \frac{(1-\varphi) + \varphi(\rho\beta)_s / (\rho\beta)_f}{(1-\varphi) + \varphi \rho_s / \rho_f} \lambda \theta = 0 \quad (17)$$

$$\frac{1}{\text{Pr} (1-\varphi) + \varphi(\rho C_p)_s / (\rho C_p)_f} \theta'' + \frac{1}{2} f \theta' = 0 \quad (18)$$

subject to

$$f(0) = 0, \quad f'(0) = 0, \quad \theta(0) = 1, \quad f'(\infty) = 1, \quad \theta(\infty) = 0 \quad (19)$$

where primes denote differentiation with respect to η .

ii) **Case of ξ large** ($\xi \gg 1$)

In this case Eqs. (9) and (10) reduce to

$$\frac{1}{(1-\varphi)^{2.5} \left[(1-\varphi) + \varphi \rho_s / \rho_f \right]} f''' + \frac{3}{2} f f'' + \frac{(1-\varphi) + \varphi(\rho\beta)_s / (\rho\beta)_f}{(1-\varphi) + \varphi \rho_s / \rho_f} \lambda \theta = 0 \quad (20)$$

$$\frac{1}{\text{Pr} (1-\varphi) + \varphi(\rho C_p)_s / (\rho C_p)_f} \theta'' + \frac{3}{2} f \theta' = 0 \quad (21)$$

subjected to the boundary conditions (19). Also, the skin friction coefficient C_f and the local Nusselt number Nu_x become

$$\frac{1}{2} \text{Re}_x^{1/2} C_f = \frac{1}{(1-\varphi)^{2.5}} f''(0,0), \quad \text{Re}_x^{-1/2} Nu_x = -\frac{k_{nf}}{k_f} \theta'(0,0) \quad (22)$$

and

$$\frac{1}{2} \text{Re}_x^{1/2} C_f = \frac{2}{(1-\varphi)^{2.5}} f''(\xi \gg 1, 0), \quad \text{Re}_x^{-1/2} Nu_x = -\frac{k_{nf}}{k_f} \theta'(\xi \gg 1, 0) \quad (23)$$

3. Aiding case. The free convection limit ($\lambda \gg 1$)

In this case, we limit the analysis to the case when $\xi \gg 1$, the other case $\xi = 0$ (full cone) being similar. To discuss the behaviour of the solution of the boundary value problems (17-19) for $\lambda \gg 1$, we introduce the following new variables

$$f(\eta) = \lambda^{1/4} F(z), \quad \theta(\eta) = \theta(z), \quad z = \lambda^{1/4} \eta \quad (24)$$

Substituting (24) into Eqs. (17) and (18), we obtain

$$\frac{1}{(1-\varphi)^{2.5} \left[(1-\varphi) + \varphi \rho_s / \rho_f \right]} F''' + \frac{3}{2} F F'' + \frac{(1-\varphi) + \varphi(\rho\beta)_s / (\rho\beta)_f}{(1-\varphi) + \varphi \rho_s / \rho_f} \theta = 0 \quad (25)$$

$$\frac{1}{\text{Pr} (1-\varphi) + \varphi(\rho C_p)_s / (\rho C_p)_f} \theta'' + \frac{3}{2} F \theta' = 0 \quad (26)$$

and the boundary conditions (19) become

$$F(0) = 0, \quad F'(0) = 0, \quad \theta(0) = 1, \quad F'(\infty) = \lambda^{-1/2}, \quad \theta(\infty) = 0 \quad (27)$$

where primes denote now the differentiation with respect to z . The boundary conditions (27) suggest an expansion for F and θ of the following form

$$F = F_0(z) + \lambda^{-1/2} F_1(z) + O(\lambda^{-1}), \quad \theta = \theta_0(z) + \lambda^{-1/2} \theta_1(z) + O(\lambda^{-1}) \quad (28)$$

where (F_0, θ_0) and (F_1, θ_1) are given by

$$\begin{aligned} \frac{1}{(1-\varphi)^{2.5} [(1-\varphi) + \varphi \rho_s / \rho_f]} F_0'''' + \frac{3}{2} F_0 F_0'' + \frac{(1-\varphi) + \varphi(\rho\beta)_s / (\rho\beta)_f}{(1-\varphi) + \varphi \rho_s / \rho_f} \theta_0 = 0 \\ \frac{1}{\text{Pr}} \frac{1}{(1-\varphi) + \varphi(\rho C_p)_s / (\rho C_p)_f} \theta_0'' + \frac{3}{2} F_0 \theta_0' = 0 \end{aligned} \quad (29)$$

$$F_0(0) = 0, \quad F_0'(0) = 0, \quad \theta_0(0) = 1, \quad F_0'(\infty) = 0, \quad \theta_0(\infty) = 0$$

$$\begin{aligned} \frac{1}{(1-\varphi)^{2.5} [(1-\varphi) + \varphi \rho_s / \rho_f]} F_1'''' + \frac{3}{2} (F_0 F_1'' + F_0'' F_1) \\ + \frac{(1-\varphi) + \varphi(\rho\beta)_s / (\rho\beta)_f}{(1-\varphi) + \varphi \rho_s / \rho_f} \theta_1 = 0 \end{aligned} \quad (30)$$

$$\begin{aligned} \frac{1}{\text{Pr}} \frac{1}{(1-\varphi) + \varphi(\rho C_p)_s / (\rho C_p)_f} \theta_1'' + \frac{3}{2} (F_0 \theta_1' + F_1 \theta_0') = 0 \\ F_1(0) = 0, \quad F_1'(0) = 0, \quad \theta_1(0) = 0, \quad F_1'(\infty) = 1, \quad \theta_1(\infty) = 0 \end{aligned}$$

Thus, from (22), we have

$$\begin{aligned} \frac{1}{2} \text{Re}_x^{1/2} C_f = \frac{1}{(1-\varphi)^{2.5}} \lambda^{3/4} [F_0''(0) + \lambda^{-1/2} F_1''(0) + O(\lambda^{-1})] \\ \text{Re}_x^{-1/2} Nu_x = -\frac{k_{nf}}{k_f} \lambda^{1/4} [\theta_0'(0) + \lambda^{-1/2} \theta_1'(0) + O(\lambda^{-1})] \end{aligned} \quad (31)$$

for $\lambda \gg 1$. It should be mentioned that Eqs. (29) describe the problem of free convection from a full vertical cone in a nanofluid.

4. Results and discussion

As we have mentioned before, the problem is formulated so that we can consider different types of nanoparticles (e.g. Cu, Al_2O_3 , TiO_2 , etc.) and water as a base fluid. However, in order to save space, we have considered here only the case of Cu nanoparticles. The thermophysical properties of the base fluid and nanoparticles are listed in Table 1. Following Aminossadati and Ghasemi (2012), we considered the range of nanoparticle fraction parameter ϕ as $0 \leq \phi \leq 0.05$ and the Prandtl number of the base fluid (water) is kept constant at $\text{Pr} = 6.7$. It can be stated that the present study reduces to that of a viscous (Newtonian) fluid when $\varphi = 0$.

The non-linear partial differential equations (9) and (10) with the boundary conditions (11) have been solved numerically for several values of the governing parameters. The derivatives with respect to ξ were discretized using the first order upwind finite differences and the resulting ordinary differential equations with respect to η were solved using *bvp4c* routine from Matlab. For marching in ξ direction a step $\Delta\xi = 0.01$ has been used, while the absolute error tolerance in *bvp4c* was $1e-9$. Also the sets (17-19), (20,21) and (29,30) of ordinary differential equations were solved numerically using the same Matlab routine (*bvp4c*). We believe this is a better numerical method than the popular Keller box method used for solving such problems, especially in obtaining the multiple (dual) solutions. Therefore, in order to validate the present numerical method, we have compared our results with those reported by Kumari et al. (1989) for two values of Pr when $\xi = 0$ (full cone) $\lambda = 0$ (forced convection) and $\phi = 0$ (Newtonian fluid) as shown in Table 2. The comparisons are found to be in very good agreement. However, in order to compare the results, we have to take in Kumari et al. (1989), $\xi = 1$ and to use the transformation $\eta = \sqrt{3}\bar{\eta}$, $f(\eta) = \frac{1}{\sqrt{3}} F(\bar{\eta})$ and $-\theta(\eta) = \Theta(\bar{\eta})$.

Figures 2 and 5 display the variation of the reduced skin friction coefficient $f''(0)$ and the reduced Nusselt number $-\theta'(0)$ for $\xi = 0$ (full cone) and $\xi \gg 1$ when $\lambda < 0$ (opposing flow) and $\phi = 0$ (regular fluid), 0.03 and 0.05. It was found that there are regions of unique solutions for $\lambda > 0$ (assisting flow), dual (upper and lower branch) solutions exist for $\lambda < 0$ (opposing flow). This happens because the forced flow and the flow due to the buoyancy are in opposite directions. The solution for each value of ϕ exists up to a critical value of λ ($\lambda_c < 0$ say) (opposing flow). Beyond this value we are unable to get the solution using the boundary layer approximations and the full Navier-Stokes equation has to be used. The upper curve for a particular value of ϕ ends at $\lambda_c (< 0)$ and the lower branch solution continues further and terminates at a certain value of $\lambda < 0$. It should be remarked that the computations have been performed increasing λ until the point where the solution does not converge ($\lambda = \lambda_c < 0$), and the calculations were terminated at that point. In both cases of $\xi = 0$ and $\xi \gg 1$, the values of λ_c decrease with the increases of the nanoparticle concentration parameter ϕ . The values of $\lambda_c < 0$ are given in Table 3 for $\phi = 0, 0.03, 0.05$, and $\xi = 0, 5$ and $\xi \gg 1$.

Figures 3 and 6 present the velocity and temperature (upper and lower branch) profiles for $\xi = 0$ (full cone) and $\xi \gg 1$ when $\lambda = -0.2$ and $\phi = 0, 0.03$ and 0.05 , which support the existence of the dual nature of the solutions presented in Figs. 2 and 5. The velocity and thermal boundary layer thicknesses increase

with the increases of the nanoparticle volume fraction parameter ϕ . This is due to the increase of the viscosity and thermal conductivity of the nanofluid with the increasing of the nanoparticles volume fraction, see Eqs. (5) and (6). A reverse flow is noticed from Figs. 3a and 6a in the case of the lower branch solution. It is worth mentioning that the lower branch solutions are unstable and the boundary layer thicknesses of these solutions are higher as for the upper branch solutions. This can be shown by performing a stability analysis, but this is out of the scope of the present paper. Such an analysis has been done by Weidman et al. (2006), Rosca and Pop (2013) and Trîmbițaș et al. (2013).

Furthermore, Figs. 4 ($\xi = 0$) and 7 ($\xi \gg 1$) illustrate the velocity and temperature profiles for $\lambda > 0$ (assisting flow) and $\phi = 0, 0.03, 0.05$. It is easy to notice that near the surface of the truncated cone there is an overshoot of the velocity profile for large values of $\lambda (> 0)$. This is in agreement with the physical phenomenon that for large values of $\lambda (> 0)$ the convective heat transfer dominates the conductive heat transfer and buoyancy is much larger than convective flow. In addition, it is seen that the velocity profiles increase with λ , while the temperature profiles decrease with $\lambda (> 0)$, which is in agreement with Fig. 8.

Figure 8 displays the asymptotic behaviour of the reduced skin friction coefficient $f''(0)$ and reduced Nusselt number $-\theta'(0)$ for $\lambda \gg 1$ when $\xi \gg 1$ and $\phi = 0, 0.03$ and 0.05 . It is further observed that there is a very good agreement between the numerical solution of Eqs. (20) and (21) and the asymptotic solution of Eqs. (29) and (30). Reduced skin friction and Nusselt number decrease with ϕ and increase with λ . The values of the coefficients $F_0''(0)$, $F_1''(0)$, $\theta_0'(0)$ and $\theta_1'(0)$ involved in Eq. (31) are given in Table 4.

Finally, Fig. 9 presents the variation of velocity profiles and temperature profiles with ξ between the two limit cases: full cone ($\xi = 0$) and ξ large ($\xi \gg 1$). One can see that both velocity and temperature profiles decrease with the increases of ξ and as a consequence the skin friction coefficient is lower and Nusselt number is higher for larger values of ξ (truncated cone), which is important in some practical applications.

5. Conclusions

The steady mixed convection boundary layer flow of a nanofluid over a vertical frustum of a cone has been theoretically studied. A frequently used nanofluid model based on formulas for thermal

conductivity and dynamic viscosity is considered. The working fluid is chosen as water with the Prandtl number of $Pr = 6.7$. The effects of the particle volume fraction parameter ϕ , the mixed convection parameter λ and the dimensionless coordinate ξ on the flow and heat transfer characteristics are determined for the Cu nanoparticles. From this investigation, some conclusions were summarized as follows:

- a. The reduced skin friction coefficient $f''(\xi, 0)$ increases due to increase in the parameter λ while it decreases due to increase in particle volume fraction parameter ϕ when $\lambda > 0$.
- b. The reduced local Nusselt number $-\theta'(\xi, 0)$ is also influenced by the particle volume fraction parameter ϕ and the mixed convection parameter λ . Thus, it increases with the increase of λ and decreases with the increase of the volume fraction parameter ϕ for positive λ . The increasing volume fraction of Cu nanoparticle increases the thermal conductivity which results in increasing of the thermal boundary layer.
- c. The nanofluid temperature increases due to increasing in the particle volume fraction parameter ϕ , while it decreases due to increase in the mixed convection parameter λ when assisting flow is considered.
- d. Dual solutions were found in the opposing flow case in the region $\lambda \in [\lambda_c, 0]$. When $\lambda < \lambda_c$ it is not possible to find a solution if the boundary approximation model is used.
- e. It was shown that the numerical method based on *bvp4c* from Matlab works very efficient for this kind of problems.

Acknowledgment

The work of the first author was supported by the Sectorial Operational Programme for Human Resources Development 2007-2013, co-financed by the European Social Fund, under the project number POSDRU/88/1.5/S/60185 with the title “Modern Doctoral Studies: Internalization and Interdisciplinarity”. The work of the corresponding author was supported from the grant PN-II-RU-TE-2011-3-0013, UEFISCDI, Romania.

References

- Aminossadati, S.M. and Ghasemi B. 2012, “Conjugate natural convection in an inclined nanofluid-filled enclosure”, *International Journal of Numerical Methods for Heat & Fluid Flow*, Vol. 22, pp. 403-423.
- Buongiorno, J. 2006, “Convective transport in nanofluids”, *ASME Journal of Heat Transfer*, Vol. 128, pp. 240–250.
- Buongiorno, J and Hu, W. 2005, “Nanofluid coolants for advanced nuclear power plants”, Paper no. 5705. In: Proceedings of ICAPP '05, Seoul, May 15-19, 2005.
- Brinkman, H.C. 1952, “The viscosity of concentrated suspensions and solutions”, *Journal of Chemistry Physics*, Vol. 20, pp. 571–581.
- Chamkha, A.J. 2001 "Coupled heat and mass transfer by natural convection about a truncated cone in the presence of magnetic field and radiation effects", *Numerical Heat Transfer, Part A*, Vol. 39, pp. 511-530.
- Mahdy, A., Chamkha, A. J. and Baba, Y. 2010, “Double–diffusive convection with variable viscosity from a vertical truncated cone in porous media in the presence of magnetic field and radiation Effects”, *Computers & Mathematics with Applications*, Vol. 59, pp. 3867-3878.
- Chamkha, A.J., Rashad, A.M. and Al-Mudhaf, H. 2012, “Heat and mass transfer from truncated cones with variable wall temperature and concentration in the presence of chemical reaction effects”, *International Journal for Numerical Methods in Heat and Fluid Flow*, Vol. 22, pp. 357-376.
- Chamkha, A.J. and Rashad, A.M. 2012, “Natural convection from a vertical permeable cone in a nanofluid saturated porous media for uniform heat and nanoparticle volume fraction fluxes”, *International Journal of Numerical Methods for Heat & Fluid Flow*, Vol. 22, pp. 1073-1085.
- Chiou, I.P. and Na, T.Y. 1980, “Laminar natural convection over a slender vertical frustum of a cone with variable surface temperature”, *The Canadian. J. Chem. Engng.*, Vol. 58, pp. 438-442.
- Choi, S.U.S. 1995, “Enhancing thermal conductivity of fluids with nanoparticles”, In: Siginer, D.A. and Wang, H.P. (eds.), *Developments and Applications of Non-Newtonian Flows*, FED, Vol. 231, 66, pp. 99–105.
- Choi, S.U.S. 2009, “Nanofluids: From vision to reality through research”, *ASME Journal of Heat Transfer*, Vol.131, Art. No. 033106.
- Choi, S.U.S., Zhang, Z.G., Yu, W., Lockwood, F.E. and Grulke, E.A. 2001, “Anomalously thermal conductivity enhancement in nanotube suspension”, *Appl. Phys. Lett.*, Vol. 79, pp. 2252-2254.
- Das, M. K. and Ohal, P. S. 2009, Natural convection heat transfer augmentation in a partially heated and partially cooled square cavity utilizing nanofluids, *International Journal of Numerical Methods for Heat & Fluid Flow*, Vol. 19, pp. 411-431.
- Das, S.K., Putra, N., Thiesen, P., and Roetzel, W. 2003, “Temperature dependence of thermal conductivity enhancement for nanofluids”, *ASME Journal of Heat Transfer*, Vol. 125, pp. 567–574.
- Das, S.K. and Choi, U.S. 2009, “A review of heat transfer in nanofluids”, In: Greene, G.A., Cho, Y.I. and Bar-Cohen, A. (eds.), *Advances in Heat Transfer*, Vol. 41, pp. 81-197.
- Das, S.K., Choi, S.U.S. and Yu, W. 2007, “*Nanofluids. Sciences and Technology*”, Wiley, New Jersey.
- Ding, Y., Chen, H., Wang, L., Yang, C.-Y., He, Y., Yang, W., Lee, W.P., Zhang, L. and Huo, R. 2007, “Heat transfer intensification using nanofluids”, *KONA*, Vol. 25, pp. 23-38.
- Eastman, J.A., Choi, S.U.S., Li, S., Yu, W. and Thompson, L.J. 2001, “Anomalously increased effective thermal conductivities of ethylene glycol-based nanofluids containing copper nanoparticles”, *Appl. Phys. Letter*, Vol. 78, pp. 718–720.

- Fan, J. and Wang, L. 2011. "Review of heat conduction in nanofluids", *ASME Journal of Heat Transfer*, Vol.133, pp. 040801 (14 pages).
- Hamilton, R.E, Fagan, T.J. and Kennedy, G. 1999, "Closed loop liquid cooling for semiconductor RF simplifier modules", *US005901037 A*.
- Kakaç, S., and Pramuanjaroenkij, A. 2009, "Review of convective heat transfer enhancement with nanofluids," *International Journal of Heat and Mass Transfer*, Vol. 52, pp. 3187–3196.
- Khanafer, K. ,Vafai K. and Lightstone M. 2003, "Buoyancy-driven heat transfer enhancement in a two-dimensional enclosure utilizing nanofluids", *Int. J. Heat Mass Transfer*, Vol. 46, pp.3639-3653.
- Kleinstreuer, C., Li J. and Koo J. 2008, "Microfluidics of nano-drug delivery" , *Int. J. Heat Mass Transfer*, Vol. 51, pp. 5590– 5597.
- Kumari, M., Pop, I. and Nath, G. 1989, "Mixed convection along a vertical cone", *Int. Comm. Heat Mass Transfer*, Vol. 16, pp. 247-255.
- Kuznetsov, A.V. and Nield, D.A. 2010, "Natural convective boundary layer flow of a nanofluid past a vertical plate", *Int. J. Thermal Sci.*, Vol. 49, pp. 243–247.
- Laforgia, D., Colangelo, G., Milanese, M. and De Risi, A. 2013, "Heat transfer medium with nanofluids for a thermodynamic solar system",*EP 2 557 373 A1*.
- Mansour, R. B., Galanis, N. and Nguyen, C. T. 2009, " Developing laminar mixed convection of nanofluids in an inclined tube with uniform wall heat flux", *International Journal of Numerical Methods for Heat & Fluid Flow*, Vol. 19, pp. 146-164.
- Maïga, S.E.B., Nguyen, C.T., Galanis, N. and Roy, G. 2004, "Heat transfer behaviours of nanofluids in a uniformly heated tube", *Superlattices & Microstructures*, Vol. 35, pp. 543-557.
- Masuda, H., Ebata, A., Teramae, K. and Hishinuma N. 1993, "Alteration of thermal conductivity and viscosity of liquid by dispersing ultra-fine particles", *NetsuBussei*, Vol. 7, pp. 227-233.
- Mahmood, T. and Merkin, J.H. 1988, "Similarity solutions in axisymmetric mixed-convection boundary-layer flow", *J. Engng. Math.*, Vol. 22, pp. 73-92.
- McCutcheon, J.W., Narum, T.N., Soo, P.P. and Liu, Y.J. 2005,"Flexible heat sink", *US006919504 B2*.
- Molla, M., Hossain, Md A. and Gorla, R.S.R. 2009, "Radiation erect on laminar natural convection boundary layer flow over a vertical wavy frustum of a cone", *J. Mech. Engng. Sci.*, Vol. 223 pp. 1605-1614.
- Nakamura, J., Kusunoki, K., Matsushita, M., Watanabe, M., Sawada, I., Fukada, H. and Tohi, S. 2010, "Plate heat exchanger used as evaporator or condenser", *WO2010013608*.
- Nield, D.A. and Kuznetsov, A.V. 2009, "Thermal instability in a porous medium layer saturated by a nanofluid", *Int. J. Heat Mass Transfer*, Vol. 52, pp. 5796–5801.
- Nield, D.A. and Kuznetsov, A.V. 2010, "The onset of convection in a horizontal nanofluid layer of finite depth", *Eur. J. Mech. B-Fluids*, Vol. 29, pp. 217-223.
- Olson, J.M. 2013, "Nanofluid and a method of making nanofluids for ground source heat pumps and other applications", *US0062555 A1*.
- Oztop, H.F. and Abu-Nada, E. 2008, "Numerical study of natural convection in partially heated rectangular enclosures filled with nanofluids", *International Journal of Heat and Fluid Flow*, Vol. 29, pp. 1326-1336.
- Pop, I. and Ingham, D.B. 2001, "*Convective Heat Transfer. Mathematical and Computational Modelling of Viscous Fluids and Porous Media*", Pergamon, Oxford.
- Rosca, A.V. and Pop, I. 2013. "Flow and heat transfer over a vertical permeable stretching-schrinking sheet with a second order sleep", *Applied Mathematics and Computation*, Vol. 60, pp. 355–364.
- Rohni, A., Ahmad, S. and Pop I. 2011, "Boundary layer flow over a moving surface in a nanofluid beneath a uniform free stream", *International Journal of Numerical Methods for Heat & Fluid Flow*, Vol. 21, pp. 828-846.

Schaefer, H.-E. 2009, "Nanoscience: The Science of the Small in Physics, Engineering, Chemistry, Biology and Medicine", Springer, Berlin.

Shinmura, T. 1996, "Heat exchanger", EP0694747 A2.

Tham, L., Nazar R. and Pop, I. 2012, "Mixed convection boundary layer flow from a horizontal circular cylinder in a nanofluid", *International Journal of Numerical Methods for Heat & Fluid Flow*, Vol. 22, pp. 576-606.

Tiwari, R.K. and Das, M.K. 2007, "Heat transfer augmentation in a two-sided lid-driven differentially heated square cavity utilizing nanofluids", *International Journal of Heat and Mass Transfer*, Vol. 50, pp. 2002–2018.

Trîmbițaș R., Grosan, T. and Pop I. 2013, Mixed convection boundary layer flow along vertical thin needles in nanofluids, *International Journal of Numerical Methods for Heat and Fluid Flow*, accepted.

Weidman, P.D., Kubitschek, D.G. and A.M.J. Davis, A.M.J. 2006, "The effect of transpiration on self-similar boundary layer flow over moving surfaces", *International Journal of Engineering Science*, Vol. 44, pp. 730-737.

Table 1. Thermophysical properties of fluid and nanoparticles (Oztop and Abu-Nada, 2008)

Physical properties	Fluid phase (water)	Cu	Al ₂ O ₃	TiO ₂
C_p (J/kg K)	4179	385	765	686.2
ρ (kg/m ³)	997.1	8933	3970	4250
k (W/mK)	0.613	400	40	8.9538
$\beta \times 10^{-5}$ (1/K)	21	1.67	0.85	0.9

Table 2. Skin friction and heat transfer coefficients for $\xi = 0$, $\lambda = 0$ and $\phi = 0$.

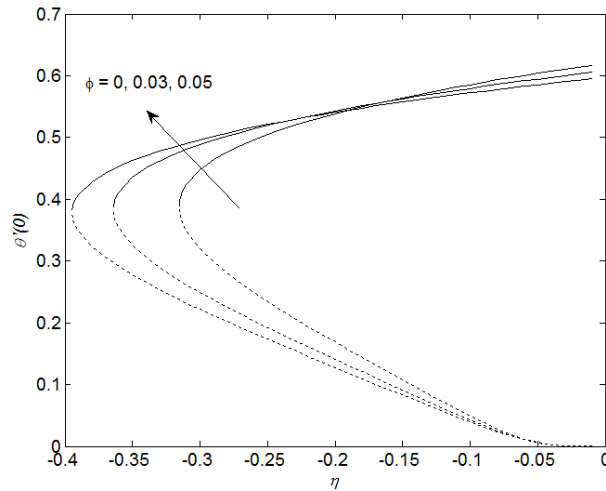
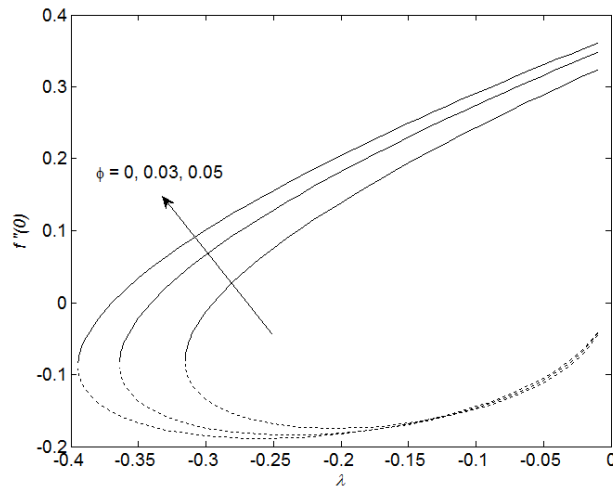
Pr	Kumari et al. (1989)		Present	
	$f''(0)$	$-\theta'(0)$	$f''(0)$	$-\theta'(0)$
0.733	1.1505	0.5158	1.150280	0.515329
6.7	1.1505	1.1025	1.150280	1.102402

Table 3. Values of λ_c .

ϕ	$\xi = 0$	$\xi = 5$	$\xi \gg 1$
0	-0.3154	-0.8500	-0.9464
0.03	-0.3640	-1.0010	-1.0921
0.05	-0.3947	-1.1421	-1.1842

Table 4. Values of $F_0''(0)$, $F_1''(0)$, $\theta_0'(0)$ and $\theta_1'(0)$ for $\xi \gg 1$.

ϕ	$F_0''(0)$	$F_1''(0)$	$-\theta_0'(0)$	$-\theta_1'(0)$
0	0.570810	0.122173	0.878720	0.173098
0.03	0.547495	0.129456	0.825799	0.187845
0.05	0.532278	0.131806	0.792171	0.194214



a)

b)

Figure 2. Variation of a) reduced skin friction coefficient $f''(0)$ and b) reduced Nusselt number $\theta'(0)$ with $\lambda (< 0)$ for $\xi = 0$ and several values of ϕ .

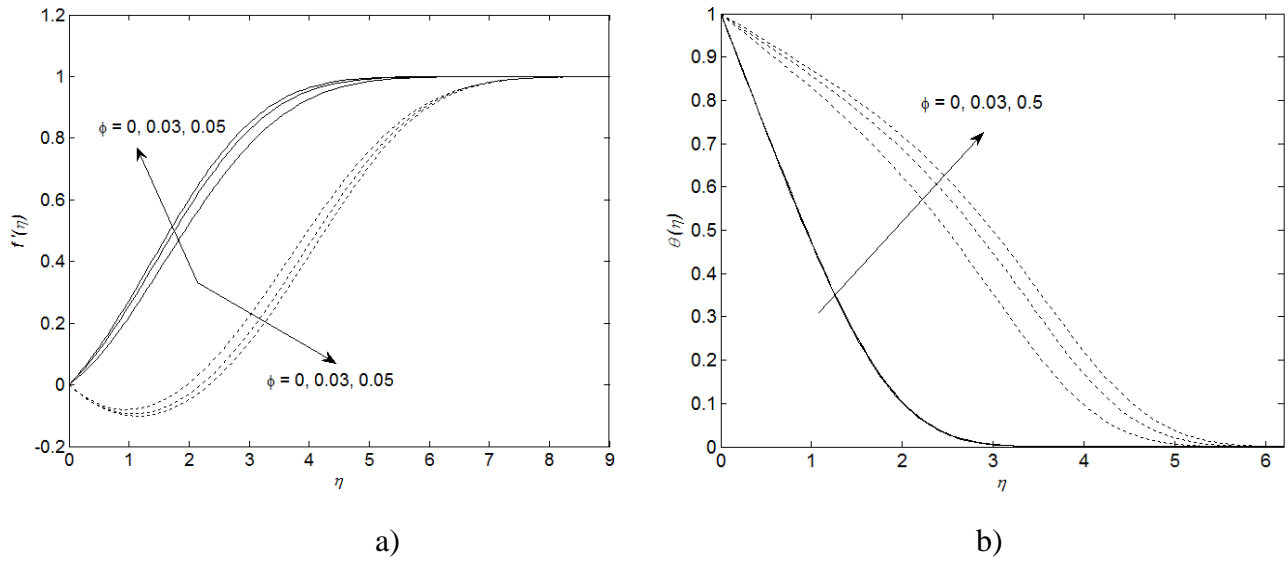


Figure 3. Upper (full line) and lower (dot line) profiles: a) velocity $f'(\eta)$ and b) temperature $\theta(\eta)$ for $\xi = 0$, $\lambda = -0.2$ (opposing flow).

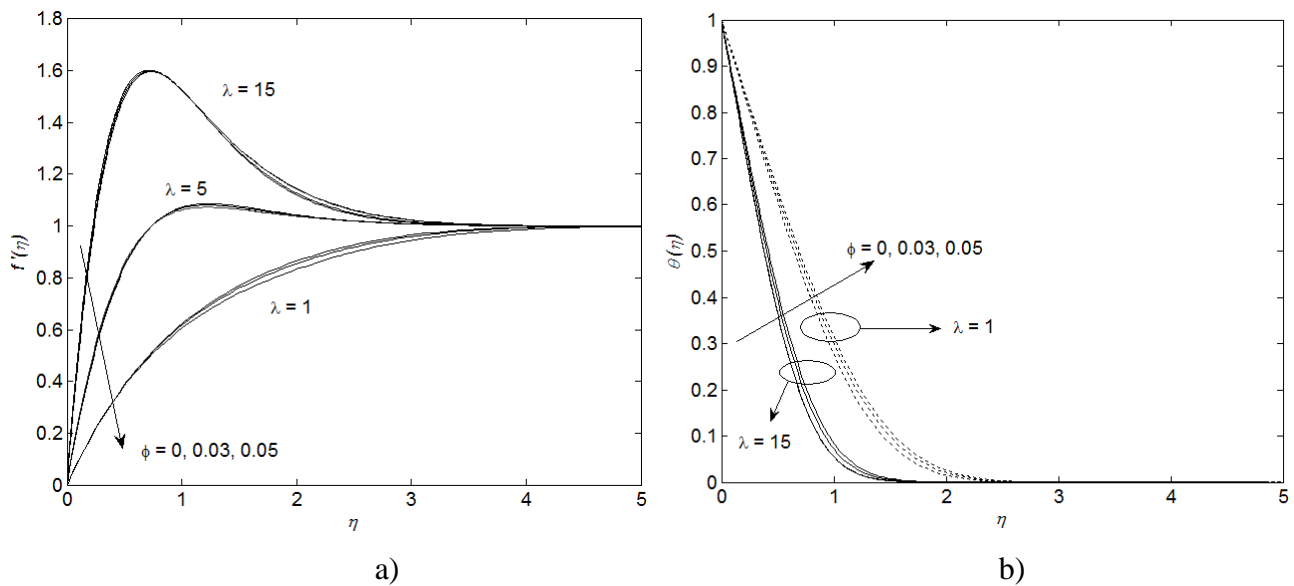


Figure 4. Profiles of a) velocity $f'(\eta)$ and b) temperature $\theta(\eta)$ for $\xi = 0$, $\lambda > 0$ (assisting flow) and several values of ϕ .

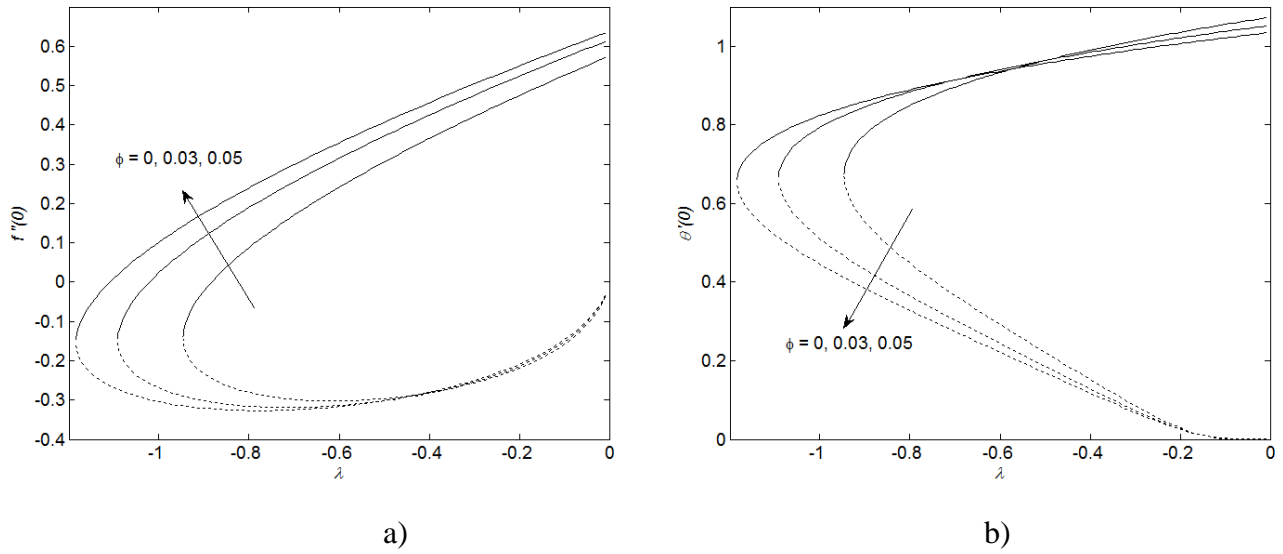


Figure 5. Variation of a) reduced skin friction coefficient $f''(0)$ and b) reduced Nusselt number $\theta'(0)$ with $\lambda (< 0)$ for $\xi \gg 1$ and several values of ϕ .

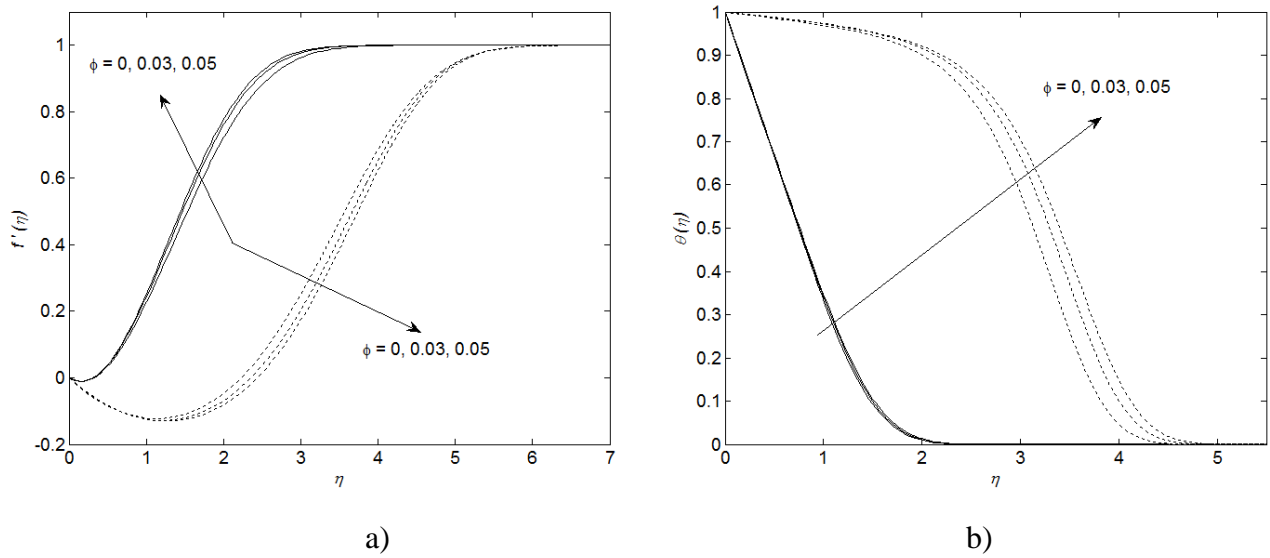


Figure 6. Upper (full line) and lower (dot line) profiles: a) velocity $f'(\eta)$ and b) temperature $\theta(\eta)$ for $\xi \gg 1$, $\lambda = -0.2$ (opposing flow).

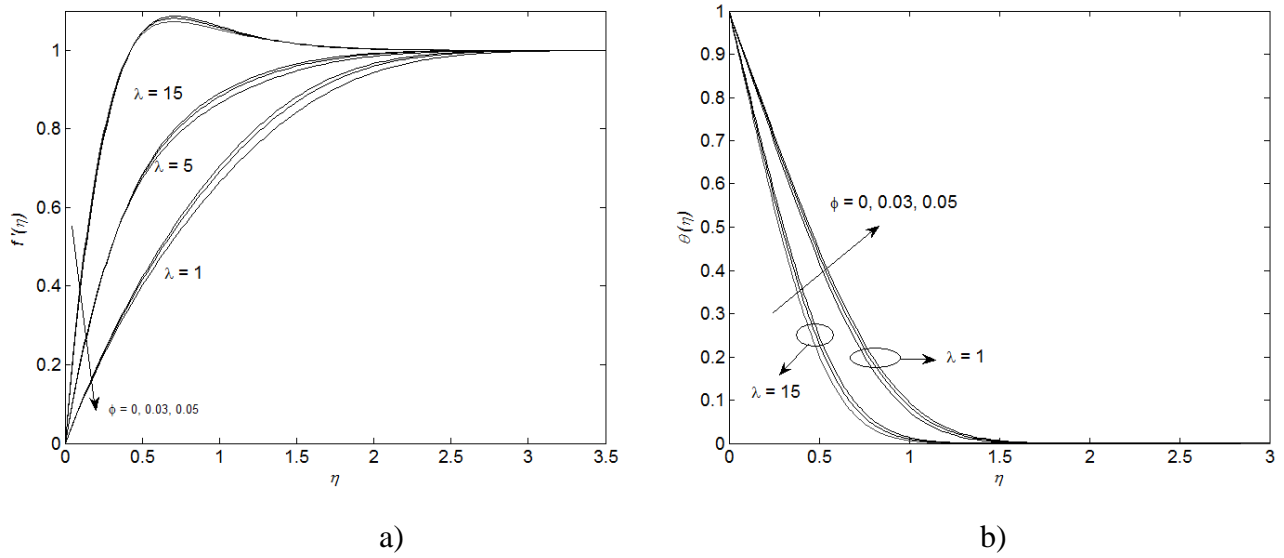


Figure 7. Profiles of a) velocity $f'(\eta)$ and b) temperature $\theta(\eta)$ for $\xi \gg 1$, $\lambda > 0$ (assisting flow) and several values of ϕ .

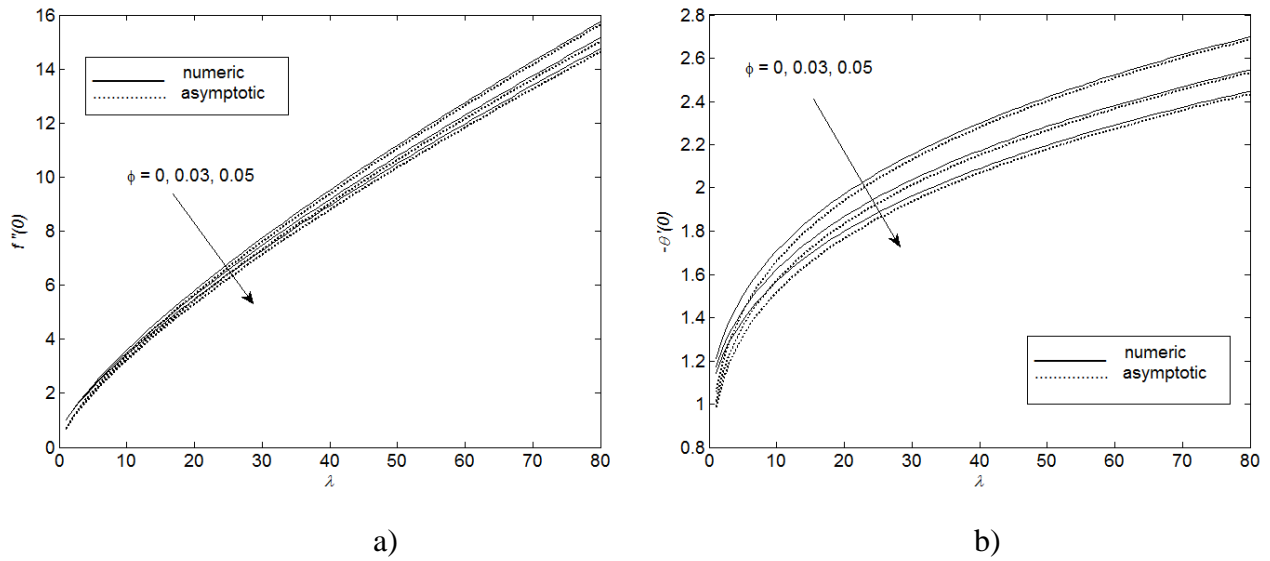
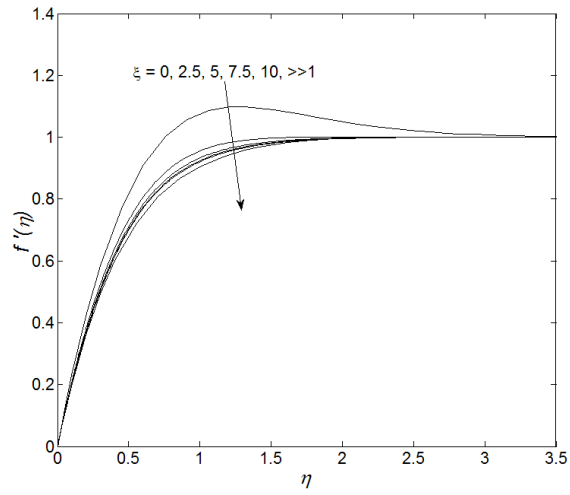
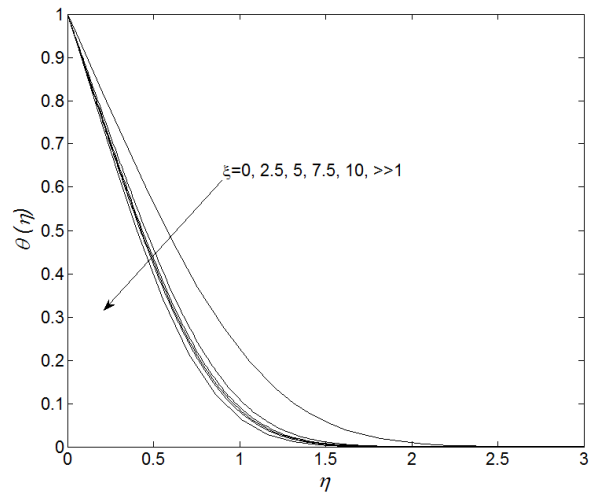


Figure 8. Variation of a) reduced skin friction $f''(0)$ and b) reduced Nusselt number $-\theta'(0)$ with $\lambda > 0$ (assisting flow) when $\xi \gg 1$ and $\phi = 0, 0.03$ and 0.05 .



a)



b)

Figure 9. Profiles of a) velocity $f'(\eta)$ and b) temperature $\theta(\eta)$ for $\phi = 0.05$, $\lambda = 5$ (assisting flow) when $\xi = 0, 2.5, 5, 7.5, 10$ and $\gg 1$.